

# Reconfigurable silicon optical filters using a dual-ring assisted Mach-Zehnder interferometer based 16×16 switch

Lin Shen, Zhazhi Guo, Liangjun Lu, Linjie Zhou\*, and Jianping Chen

State Key Laboratory of Advanced Optical Communication Systems and Networks, Department of Electronic Engineering, Shanghai Jiao Tong University, Shanghai 200240, China

Author e-mail address: ljzhou@sjtu.edu.cn

**Abstract:** We demonstrate high-order silicon optical filters based on cascaded dual-ring assisted Mach-Zehnder interferometers in a 16×16 switch chip. The filter central wavelength and bandwidth are thermally tunable with the out-of-band rejection ratio >26 dB.

**OCIS codes:** (230.0230) Optical devices, (230.7408) Wavelength filtering devices

## 1. Introduction

Reconfigurable optical filters are the basic and fundamental devices for photonic signal processing in both digital and analog optical systems. It is highly demanded for the flexible tunability of filter wavelength and optical bandwidth to adapt for multiple applications. In the past decade, silicon photonic devices have been widely studied and they provide the potential to build low-cost large-scale photonic integrated circuits. Several reconfigurable optical filters have been developed by cascading multiple stages of Mach-Zehnder interferometers (MZI) or microring resonators (MRR) [1-3].

In our previous work, we have investigated a dual-ring assisted MZI (DR-MZI) based switch element (SE) and implemented a 16×16 non-blocking silicon optical switch chip using this switch element [4, 5]. The DR-MZI can work as a second-order optical filter by properly tuning the resonance wavelength. Here, we experimentally demonstrate a silicon optical bandpass filter based on cascaded DR-MZIs. Both the filter central wavelength and the optical bandwidth are tunable.

## 2. Device structure and working principle

Figure 1(a) presents the schematic structure of the DR-MZI composed of a symmetric MZI coupled with a MRR in each arm. Both of the MRRs are integrated with TiN microheaters for low-loss thermo-optic (TO) phase tuning. Compared to a regular MZI structure, this DR-MZI design reduces the device size and the power consumption in changing the switch state. For the DR-MZI, when the two MRRs resonate at the same wavelength, light is transmitted to the cross port with a flat spectral response. Thus, the DR-MZI is at the “cross state”. As we red-shift one of the MRRs by TO tuning, the spectrum exhibits a deep notch at the cross port and a peak at the bar port around the resonance wavelength. The DR-MZI goes into the “bar state”. In fact, the DR-MZI essentially works as a second-order optical add-drop filter. As shown in Fig. 1(b), the optical bandwidth is enlarged with the increasing wavelength detuning. However, the in-band ripple also becomes more significant when the two resonances are far apart, which degrades the filter performance.

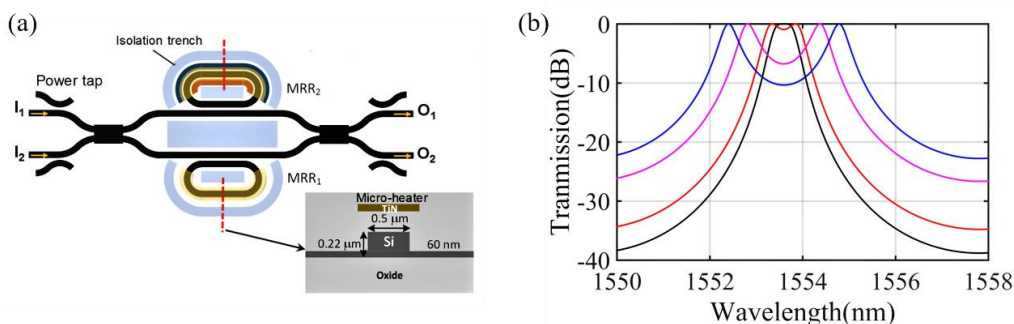


Fig. 1 (a) Schematic structure of the 2×2 DR-MZI. (b) Simulated transmission spectra of the DR-MZI when the resonances of the two MRRs are gradually separated from each other.

High-order optical filters made up of cascaded DR-MZIs have much more flexible tuning in passband spectral shape. Figure 2(a) shows the topological architecture of the 16×16 silicon optical switch, consisting of 56 DR-MZI SEs. The details of the chip design can be found in Ref. [4]. Figure 2(b) shows the photo of the packaged chip. As

each light path goes through seven stages of DR-MZIs, a highest 14<sup>th</sup>-order optical filter can be realized in principle. The filter order can be changed by setting the number of “bar state” SE along the light path.

We used the transfer matrix method to analyze the cascaded DR-MZIs. Figures 2(c) and 2(d) show the simulated spectra of seven cascaded DR-MZIs, configured as the fourth- and sixth-order bandpass filters, respectively. In order to obtain a “box”-like filter spectrum, we finely tune the resonances of the MRRs to ensure that one of the DR-MZIs has a narrow bandwidth but with high peak transmission while the others have a gradually broadened bandwidth. As can be seen, the sixth-order bandpass filter has a faster roll-off than the fourth-order filter. It should be noted that the insertion loss increases with the broadened optical passband.

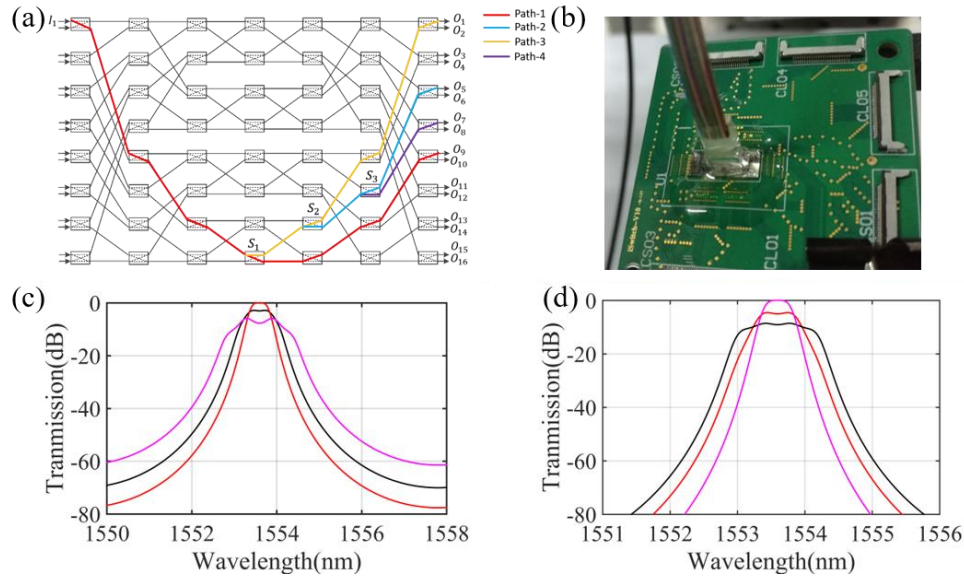


Fig. 2 (a) Architecture of the 16×16 switch matrix. (b) Photo of the home-packaged switch chip. (c) and (d) Simulated transmission spectra of (c) the fourth-order filter, and (d) the sixth-order filter with bandwidth tuning.

### 3. Experimental results

To verify the concept, we measured the 16×16 optical switch reconfigured as the second-, fourth-, and sixth-order bandpass filter. The light paths taken in the measurement are labelled in Fig. 2(a). At the initial state, the SEs along Path-1 are all tuned to the “cross state”, and thus light from  $I_1$  is routed to  $O_9$ . With TO detuning the two MRRs in  $S_1$  to change it to “bar state” and keeping the other SEs at the “cross state”, the Path-3 then presents a second-order bandpass spectrum. If we also detune the MRRs in  $S_2$ , the output  $O_5$  in Path-2 presents a fourth-order bandpass spectrum. To realize a sixth-order bandpass filter,  $S_3$  can be switched to the “bar state” together with  $S_1$  and  $S_2$ , and in this case, the optical path is changed to Path-4.

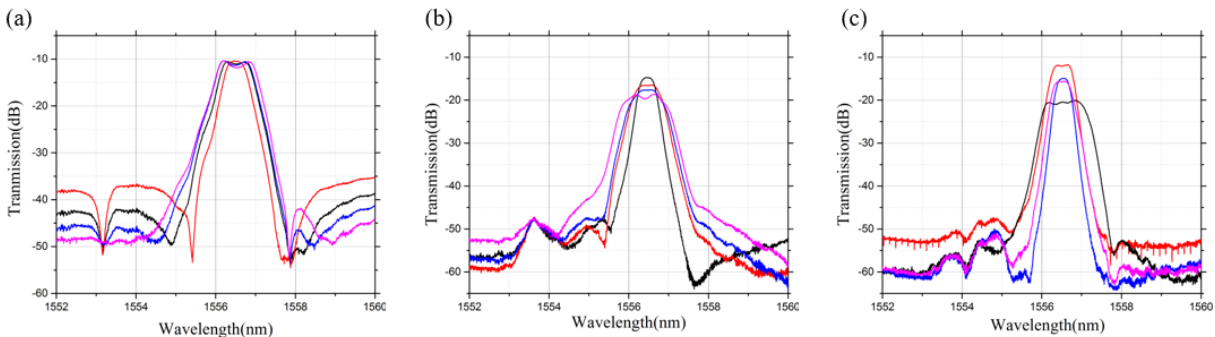


Fig. 3 Measured passband spectra for (a) the second-order, (b) the fourth-order, and (c) the sixth-order filters. In each filter configuration, the passband width is tuned with the in-band ripple kept below 1 dB.

Figures 3(a)-3(c) show the measured output spectra from Path-3, Path-2, and Path-4, showing the second-, fourth-, and sixth-order bandpass filtering properties, respectively. The bandwidth of the second-order filter is

adjusted by increasing the heating power on one MRR in  $S_1$  and decreasing the heating power on the other MRR. Thus, the filter central wavelength is fixed. The bandwidth of the fourth- and sixth-order filters is tuned by using the method described in the simulation part. As can be seen, the passband width can be tuned a little bit while the in-band ripple is kept below 1dB.

Table 1 lists the extracted 3-dB bandwidth, out-of-band rejection (OBR) and roll-off values for the three optical filters. It can be seen that the higher the filter order is, the larger the optical bandwidth tuning range is. With the increasing filter order from 2 to 6, the OBR is improved from ~26 dB to ~33 dB, and the roll-off rate is also increased from ~29 dB/nm to ~85 dB/nm.

Table 1. The extracted performance parameters of multiple high-order optical filters

Orders	Max. 3-dB BW	Min. 3-dB BW	In-band ripple	OBR	Roll-off
2	0.94 nm	0.55 nm	<1 dB	~26 dB	~29 dB/nm
4	1.12 nm	0.42 nm	<1 dB	~29 dB	~51 dB/nm
6	1.09 nm	0.37 nm	<0.95 dB	~33 dB	~85 dB/nm

Next, we measured the central wavelength tunability of the filter. Figure 4 shows the measured transmission spectra of the sixth-order filter when the central wavelength is red-shifted by 4.5 nm. The heating power to each MRR is linearly increased with the same rate, so that the shape of passband remains relatively identical upon wavelength shifting. The free spectral range (FSR) of the MRR is 8.5 nm, which means that the filter central wavelength can be tuned by over a half of FSR.

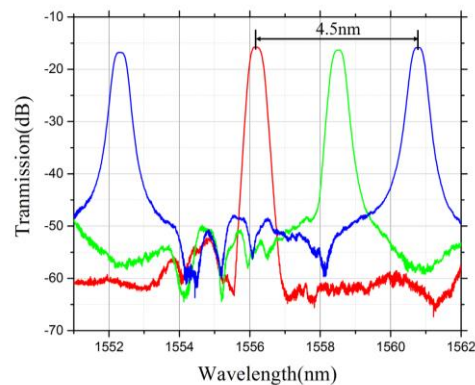


Fig. 4 Demonstration of the filter central wavelength tuning for the sixth-order optical filter.

#### 4. Conclusion

We have experimentally demonstrated a TO reconfigurable silicon optical filter using a  $16 \times 16$  DR-MZI switch chip. With a properly chosen light path, the chip can be reconfigured to optical filters with various orders. Preliminary measurement on the second-, fourth-, and sixth-order filters reveals that the bandwidth of the filter can be tuned from 0.37 nm to 1.12 nm and the OBR can exceed 26 dB with 1 dB in-band ripple. The central wavelength can be tuned to cover one half of the FSR. These results represent a significant step towards the realization of a reconfigurable optical filter based on a programmable large-scale switch chip.

#### 5. References

- [1] H. Jayatileka et al., "Automatic tuning and temperature stabilization of high-order silicon Vernier microring filters," *Opt. Fiber Commun. Conf.*, (2017)
- [2] J. R. Ong et al., "Ultra-high-contrast and tunable-bandwidth filter using cascaded high-order silicon microring filters," *IEEE Photon. Technol. Lett.* **24**, 1543-1546 (2013).
- [3] Y. Ding et al., "Bandwidth and wavelength-tunable optical bandpass filter based on silicon microring-MZI structure," *Opt. Express* **29**, 6462-6470 (2011).
- [4] Z. Guo et al., "16x16 Silicon optical switch based on dual-ring assisted Mach-Zehnder interferometers" *J. Lightwave Technol.*, under revision (2017).
- [5] L. Lu et al., "Low-power  $2 \times 2$  silicon electro-optic switches based on double-ring assisted Mach-Zehnder interferometers," *Opt. Lett.* **39**, 1633-1636 (2014).
- [6] L. Chen et al., "Compact bandwidth-tunable microring resonators," *Opt. Lett.* **32**, 3361-3363 (2007).